Effect of the Manufacturing Conditions on the Structure and Performance of Thin-Film Composite Membranes

Rui-Xin Zhang,[1] Johan Vanneste,[1] Lore Poelmans,[1] Arcadio Sotto,[2] Xiao-Lin Wang,[3] Bart Van der Bruggen[1]

[1]*Department of Chemical Engineering, Laboratory for Applied Physical Chemistry and Environmental Technology, Katholieke Universiteit Leuven, W. de Croylaan 46, Leuven B-3001, Belgium*
[2]*Department of Chemical and Energetic Technology, Rey Juan Carlos University, Madrid, Spain*
[3]*State Key Laboratory of Chemical Engineering, Department of Chemical Engineering, Tsinghua University, Beijing 100084, China*

Received 4 August 2011; accepted 22 November 2011
DOI 10.1002/app.36542
Published online in Wiley Online Library (wileyonlinelibrary.com).

ABSTRACT: A systematic investigation of the influence of the manufacturing conditions on the structure and performance of thin-film composite (TFC) membranes is presented for polyamide (PA) supported by poly(ether sulfone) (PES). The TFC membranes were composed of an ultrathin PA layer synthesized by interfacial polymerization on top of a porous PES support layer formed by immersion precipitation. For the PES support layer, the role of the wetting pretreatment, initial casting film thickness, and relative air humidity were studied. Assuming a strong correlation between the thermodynamics and the hydrodynamics of the casting process, we derived new insights from scanning electron microscopy images and the experimental data. In view of optimization of the flux through the membranes, a wetting pretreatment should be avoided. Important polymer savings were obtained without a loss of performance through a decrease in the casting thickness in combination with the use of a very smooth support. Last but not least, a high air humidity during casting was found to inhibit the formation of a dense, defect-free skin layer. For the PA layer, the interfacial polymerization method, the drying method, and the curing time were studied. The clamping of the membrane in a frame with one side in contact with the piperazine (PIP) solution and the other side to the air yielded the highest membrane flux and rejection with the lowest use of PIP and trimesoylchloride solution. Because of the absence of a uniform PIP solution layer for some drying methods, nodular PA structures could be observed in the macrovoids of the underlying PES layer because of hexane intrusion; this resulted in a dramatic decrease in the flux. Moreover, the omission of the drying step did not result in a significant loss of performance and enhanced the ease of operation. Finally, a curing time of 8 min was found to be optimal. © 2012 Wiley Periodicals, Inc. J Appl Polym Sci 000: 000–000, 2012

Key words: polyamides; poly(ether sulfones); processing; synthesis

INTRODUCTION

Thin-film composite (TFC) membranes are comprised of an ultrathin film typically made of polyamide (PA); this is coated over a porous support membrane.[1–3] TFCs have been widely used in a variety of applications, including the desalination of brackish water and seawater, freshwater softening, organic removal, ultrapure water production, and advanced wastewater purification.[4–9] The main advantage of TFC membranes is that each layer (porous support and thin film) can be optimized independently to achieve the maximum strength, stability, and desired separation performance.

The immersion precipitation process (nonsolvent-induced phase separation) is recognized as the most practical method for synthesizing porous support membranes. In this method, a polymer dissolved in an appropriate solvent is cast onto a suitable support and then immersed in a precipitation bath containing a nonsolvent.[10,11] Precipitation is induced by the exchange of a solvent and nonsolvent, and ideally, a thin dense top layer with a porous sublayer is formed in the end. The key factors that influence membrane formation by phase inversion include the choice of the solvent/nonsolvent system, the composition of the polymer solution, the composition of the coagulation bath, and the manufacturing conditions.[3,9,11–19]

Interfacial polymerization is commonly used to coat an ultrathin PA films on a porous support membrane. Polycondensation occurs between two very reactive monomers (i.e., amine and acid chloride) at the interface of two immiscible solvents.[10] The porous support membrane is immersed in an aqueous amine solution at first and then immersed in an acid chloride organic solution. These two monomers react with each other to form an ultrathin dense barrier layer on the surface of the support membrane. Heat treatment (curing) is usually applied to

Correspondence to: B. Van der Bruggen (bart.vanderbruggen@cit.kuleuven.be).

complete the dehydration and promote the additional crosslinking of PA. The key factors in interfacial polymerization include the choice of the two monomer–solvent combinations, the composition of both phases, and the manufacturing conditions.[3,9,17,20,21]

This article focuses on the effect of the manufacturing conditions of both the poly(ether sulfone) (PES) support and the PA layer on the structure and performance of the composite membrane. Particular attention will be paid to the elucidation of the underlying mechanism of the effects and the consequences for an industrial process.

Until this point, several manufacturing conditions have been studied and have been proven to have a significant effect on membrane performance. For example, to make porous support membranes, most research has focused on the support material of the sublayer (with and without nonwoven support),[18] the thickness of the polymer casting film,[11] the relative air humidity,[18] the temperature (of the polymer solution and precipitation bath),[3,11,18] and the evaporation time (a combination of processes). To manufacture ultrathin PA films, researchers have investigated the effects of the sublayer structure and properties,[9] immersion time,[17] interfacial polymerization temperature and time,[3] and heating (curing) temperature and time[3] on the performance of PA films.

Although specific manufacturing conditions have already been studied in the past, there are still several conditions that have not gotten any attention or for which the underlying mechanism of the effect is still unclear. Boussu et al.[18] found that a high air humidity before casting had detrimental effects on the membrane performance and reproducibility. They also found a large impact of a wetting pretreatment on the resultant flux, but they did not provide an explanation for these effects. By combining knowledge of the thermodynamics and especially the hydrodynamics of the manufacturing process with scanning electron microscopy (SEM) imagery and experimental data, for the first time, we derived a comprehensive explanation for the effects of a nonwoven fabric wetting pretreatment, the initial casting film thickness, and the relative air humidity on the resulting PES support structure and performance. Several optimal casting conditions and possible further improvements were identified. For the PA layer synthesis, the effects of three different interfacial polymerization methods, seven different drying methods, and the curing time were studied. Also, some procedures were clearly more advantageous than others.

EXPERIMENTAL

Material

PES beads (Radel-100, Solvay Speciality Polymers Germany GmbH, Düsseldorf, Germany), *N*-methyl-2-pyrrolidone (NMP; 99.5%, Sigma Aldrich, St. Louis, MO, USA), distilled water, and a nonwoven fabric layer (FO2471, Viledon, Weinheim, Germany) were used to manufacture the PES support layers. PA thin films were formed by the diamine monomer piperazine (PIP; 99%) and the acid chloride monomer trimesoylchloride (TMC; 98%); these were provided by Across Organics (Geel, Belgium). The solvents used for PIP and TMC were distilled water and hexane (technical, Nyssens Graphics, Belgium), respectively. For the membrane performance tests, magnesium sulfate ($MgSO_4$) supplied by Sigma-Aldrich (St. Louis, MO, USA), was used.

Synthesis of the PES support membranes

For the reference membrane, the standard manufacturing method was as follows. A homogeneous PES casting solution was prepared by the dissolution of 25 g of PES beads in 81.75 mL of NMP in an airtight glass bottle at room temperature for 1 day with continuous stirring, and air bubbles were removed before casting. Before we cast the membrane, the nonwoven fabric layer was taped onto a glass plate without pretreatment. A thin film of PES solution with a thickness of 200 μm was spread over the nonwoven fabric layer with a casting knife in an atmosphere with a controlled relative air humidity (40%). The casting film was then immediately immersed in a nonsolvent bath containing distilled water at room temperature to initiate phase separation. After 15 min, the asymmetric porous membrane was removed from the nonsolvent bath, washed thoroughly with distilled water, and stored in a distilled water bath.

The influence of the nonwoven fabric wetting pretreatment was studied by the variation of the concentration of the NMP solution applied on the fabric surface. For the purpose of understanding the effect of the initial casting film thickness and the relative air humidity, different heights of the casting knife (100, 150, 200, and 250 μm) and different relative air humidities were used during manufacturing.

Synthesis of the TFC PA membranes

TFC PA membranes were formed by interfacial polymerization. The standard manufacturing method of the reference membranes was as follows. The PES support membrane was clipped between two thick frames; this allowed the active side to be in contact with the solutions and the backside to be exposed to air. A 4% aqueous PIP solution was poured into the thick frame; after we waited 30 s, the excess PIP solution was drained off the surface for 30 s and was then removed by a rubber wiper until no visible excess solution remained. The membrane was then immersed in a 0.5% TMC solution in hexane for 30 s; this resulted in an ultrathin PA layer on the

membrane surface. The excess hexane solution was poured off, and the membrane, together with the frame, was heated in a vacuum oven at 60°C to remove the residual hexane and promote crosslinking. Finally, the membrane was rinsed and stored in distilled water before testing.

To study the influence of the interfacial polymerization method on the resulting membrane structure and performance, three methods were applied in the experiment (see the Effect of the Interfacial Polymerization Method section). To examine the role of the drying method in the removal of excess amine solution, seven generally used approaches were studied. Finally, the heating (curing) time was investigated.

Characterization of the membranes

The intrinsic water permeability and salt rejection were tested in a dead-end filtration module (HP4750 stirred cell, Sterlitech Corp., Kent, WA, USA), which was placed on a magnetic stirring platform. The vessel, filled with 250 mL of feed solution, was pressurized by nitrogen gas. The permeate was collected in a graduated cylinder for a certain time interval. The active area of the membrane was 14.6 cm^2. All tests were performed at 20 bar and room temperature ($\sim$ 20°C). Before testing, the membranes were compacted to obtain a steady permeate flux.

The pure water flux was obtained by the division of the permeate volume by the membrane area and time. The intrinsic water permeability (A) was calculated by dividing the pure water flux (J_w) by the applied static pressure (ΔP):

$$A = J_w/\Delta P$$

A 2000-ppm $MgSO_4$solution was used as a feed solution in all cases. The observed $MgSO_4$ rejection (R) was calculated from the following equation:

$$R = 1 - c_p/c_f$$

where c_p is the conductivity of the permeate solution and c_f is the average conductivity of the initial feed and the final concentrated solution. Three membrane coupons of the same membrane sheet were tested. For each manufacturing procedure, three membrane sheets were prepared. Therefore, the values of the pure water flux and salt rejection for each procedure were the averages of nine experimental results.

To investigate the influence of each manufacturing parameter on the membrane performance, student t tests and analyses of variance (ANOVAs) were performed to assess whether there was a statistical difference among the different membranes. The student t test was used to compare the means of two groups. The means of three or more groups were compared with ANOVA; this prevented the error generated in the performance of multiple t tests. The reference membranes were made by the standard procedure described in the sections on the Synthesis of the PES Support Membranes and Synthesis of the TFC PA Membranes. Other membranes were manufactured by the variation one parameter at a time.

Before performing the student t test and ANOVA, we measure the equality of variances with Levene's test. When the significance value of a Levene's test is more than 0.05, the equal variances assumed test should be performed. Otherwise, the equal variances not assumed test is used. The null hypothesizes of the t test and ANOVA constituted the situation in which there was no difference between the reference membrane and other membranes in this study. The two-tailed p value was used in our work. A p value equal to or less than 0.05 was considered statistically significant; this means that the null hypothesis was rejected, and the methods differed from one another. All of the statistical analysis in our work was performed with SPSS (Statistical Package for the Social Sciences) statistical software (IBM, New York, USA).

The cross sections and surface morphologies of the membranes were inspected by SEM (Philips XL30 FEG SEM, Eindhoven, Netherlands). To obtain a clear cross section, wet membrane samples were dipped in liquid nitrogen and cracked. After drying overnight, the samples were sputtered with gold. The average thickness of the membrane was measured at 12 different positions for each sample.

RESULTS AND DISCUSSION

Preparation of the porous support membranes

Effect of the nonwoven fabric pretreatment

To prevent the casting solution from penetrating the nonwoven support layer, the support can be wetted with solvent, or the casting speed can be increased. The FO2471 fabrics were used as a support layer. One group of membranes was cast after the fabrics were wet with different concentrations of NMP in distilled water at a speed of 3.81 m/h. The concentrations of NMP were 100, 90, 80, 70, and 60%, respectively. The other group was fabricated onto nonwetted fabrics at a speed of 32.62 m/h. All of these methods prevented the penetration problem. Representative SEM images of the cross section and bottom morphology for the membranes with and without pretreatment are shown in Figure 1.

For the cross section, the upper parts of both membranes appeared similar. However, the structures of the bottom parts were quite different from each other. Fingerlike macrovoids in the membranes without wetting pretreatment reached the backside of the membrane. However, in the membranes with

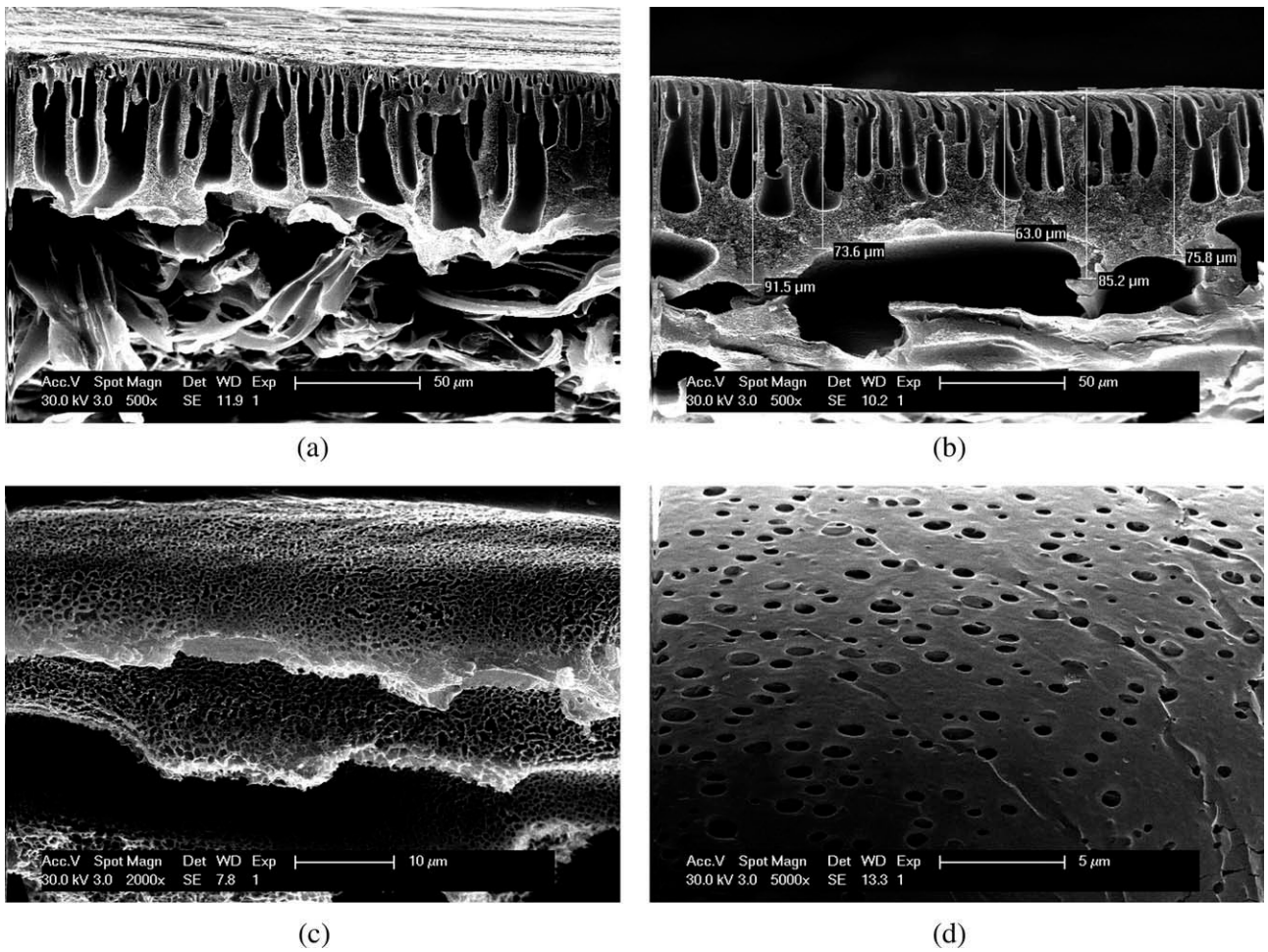

Figure 1 SEM micrographs of PES membranes prepared with and without the wetting pretreatment: cross sections of the membranes (a) without wetting pretreatment and (b) with pretreatment (100% NMP). Bottom morphology of the membranes (c) without wetting pretreatment and (d) with pretreatment (100% NMP).

wetting pretreatment, a denser and spongelike structure was formed beneath the fingerlike macrovoids. The bottom morphology [Figs. 1(c,d)] revealed that the membrane without wetting had a lower porosity than the ones with the pretreatment step. When the fabric was wetted with NMP, a barrier of solvent film was formed on the bottom; this greatly delayed the nonsolvent diffusion into the casting solution. The film acted as a reservoir of solvent. The availability of solvent at the bottom was higher and limited the influx of nonsolvent. As a result, demixing was delayed. The concentration of solvent at the bottom was higher, and the concentration gradient of the nonsolvent was, therefore, lower than that without wetting. Large-concentration gradients are considered to be one of the main driving forces for macrovoid formation. As a result, a lower concentration gradient will lead to a thicker spongelike structure on the bottom.

The SEM images of the membranes cast on fabrics wetted with 60, 70, 80, and 90% NMP were similar to the images of the membranes with 100% NMP. Because we removed the excess wetting solution from the fabric surface with a tissue, the solution in and under the fabric was very limited. Although there was some nonsolvent (water) in the wetting layer, the quantity of the water was not great enough to exchange with the solvent inside the casting film.

Figure 2 demonstrates the influence of different nonwoven fabric pretreatments on the pure water flux and salt rejection of $MgSO_4$. The results are plotted with average values, and the standard deviations of the measured values are indicated by the error bars. The comparison shows that there was no significant differences among the performances of the membranes cast on wetted fabrics with 60, 70, 80, or 90% NMP. The pure water flux of the membrane without wetting pretreatment (28.00 L m^{-2} h^{-1}) was, however, significantly higher than the flux of the membrane that underwent the wetting step (17.33 L m^{-2} h^{-1}, $p < 0.004$). However, the difference in salt rejection between the two membranes was not clear ($p < 0.178$). This means that without wetting pretreatment, a membrane was obtained with a flux that was, on average, 65% higher and a very similar salt rejection

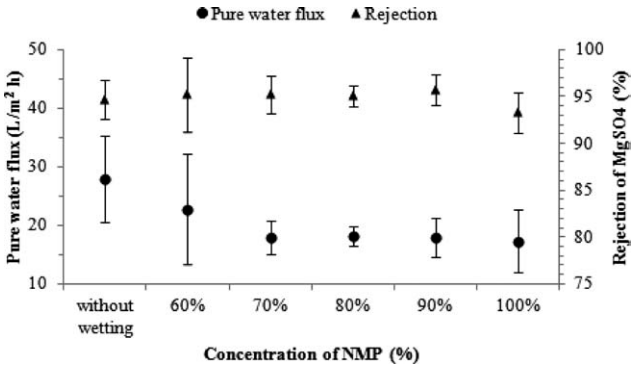

Figure 2 Effect of different nonwoven fabric pretreatments on the performance of the membranes.

(with a 1.5% difference).The performance of these membranes was consistent with the observation that the salt rejection depended on the surface structure and the morphology of the TFC membrane, and the pure water flux greatly depended on the structure of the support membrane. For the membranes cast on the fabrics wetted with 60, 70, 80, 90, and 100% NMP, their similar structures led to similar performances. With the same solvent and nonsolvent exchanging conditions on the top surface of membranes, the membranes with and without the wetting pretreatment step had similar surface structures; this resulted in similar salt rejections. In the membrane without pretreatment, the fingerlike macrovoids across the entire thickness resulted in a significantly higher flux than in the membranes with pretreatment.

This study indicated that an increase in the casting speed successfully prevented the casting solution from penetrating through the support. Moreover, in this way, a membrane was obtained with a much higher permeability and a similar rejection. Therefore, unless a dense membrane structure is desired or the viscosity of the solution is too low, a wetting pretreatment should be avoided.

Effect of the initial casting film thickness

Representative SEM images of membranes cast with different initial thicknesses are shown in Figure 3. In Figures 3(a–c) and 1(a), the membranes are shown in cross section, and all of these images show a similar porous and fingerlike structure across the entire thickness. However, it is obvious that the final thicknesses of the membranes dramatically decreased as the initial thickness decreased. The image analysis suggested final active thicknesses (above the fabrics) of the membranes on the order of 75.18 $\pm$ 6.07, 67.45 $\pm$ 4.46, 27.92 $\pm$ 3.09, and 14.04 $\pm$ 2.06 μm for initial thicknesses of 250, 200, 150, and 100 μm, respectively. The respective decreases in thickness were around 69.93 $\pm$ 0.024, 66.28 $\pm$ 0.022, 81.39 $\pm$ 0.021, and 85.96 $\pm$ 0.021%.

The decrease in thickness was caused by the hydrodynamic pressure generated by the nonsolvent influx. The faster demixing occurred or, in other words, the higher the concentration gradients in the system were, the higher the generated hydrodynamic pressure and the resulting membrane compaction were. The decrease in the concentration gradient along the membrane thickness and the corresponding decrease in hydrodynamic pressure were the main reasons an asymmetric membrane structure with a dense skin layer was formed. It, therefore, also seemed logical that the percentage decrease in thickness increased roughly inversely with the starting thickness from 69.93 to 85.96% for casting thicknesses of 250 to 100 μm. Averaged over the thickness of the casting film, a thinner casting film was subject to higher hydrodynamic pressures; this resulted in more membrane compaction.

The SEM images in Figure 3(d,e) display the surface morphology of the membrane cast with an initial thickness of 100 μm. The PES membrane did form on the nonwoven fabric but with a defective structure. This was due to the randomly arranged fibers in the nonwoven fabrics, which constituted a very rough support layer. To prevent these defects, an increase in the thickness or the use of a smoother support was necessary. Figure 3(f) shows the surface morphology of the membrane cast with a 150-μm thickness. This membrane seemed to be defect-free, but the significantly lower salt rejection (Fig. 4) compared to that of the 200-μm membrane could have indicated that there were indeed some defects.

The experimental results of the pure water flux and salt rejection are presented in Figure 4. The observed water flux increased as the initial thickness decreased (250 $>$ 200 $>$ 150 μm), whereas the observed salt rejection decreased in the order of 250 $>$ 200 $>$ 150 μm. For the membrane cast with a thickness of 100 μm, because of the defective surface, there was no experimental result. The statistical analysis (ANOVA) results indicate that there was no significant difference in the water flux and salt rejection between the membranes with initial thicknesses of 250 and 200 μm ($p < 0.568$). This means that the same performance was achieved with 20% less polymer solution through a decrease in the casting thickness from 250 to 200 μm. The performance of the membrane cast with a thickness of 150 μm was significantly different from those of the other membranes ($p < 0.000$). Although the use of the polymer solution was reduced by an additional 25% (40% in total relative to the 250-μm membrane), the large decrease in the rejection of this membrane in combination with a minor increase in the flux relative to the 200-μm membrane might decrease the application range of this membrane.

We concluded that to ensure a defect-free surface and to minimize the use of polymer solution, a film

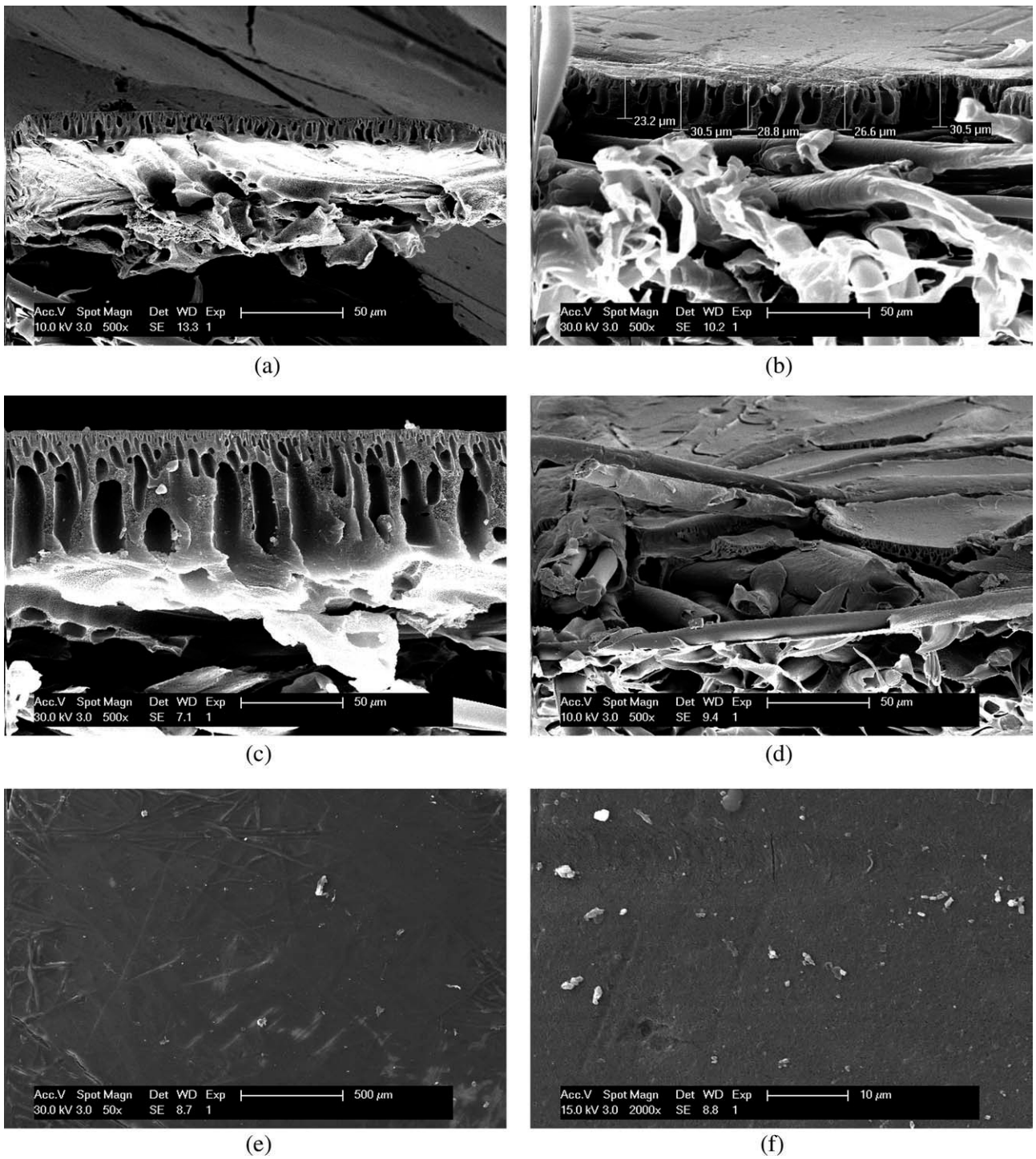

Figure 3 SEM micrographs displaying the cross sections and surface morphologies of membranes cast from different initial thicknesses: cross section of membranes with (a) 100, (b) 150, and (c) 250-μm initial thickness and surface morphologies of the membranes with (d,e) 100 and (f) 150 μm initial thicknesses.

thickness of 200 μm seems optimal. It might be possible to further reduce the membrane thickness if a much smoother support structure is used. In conjunction with decreasing the membrane thickness, prewetting can be applied to obtain a denser and more rigid membrane structure that is less prone to defect formation.

Effect of the relative air humidity

To investigate the effect of the relative air humidity on the structure and performance of membranes, four groups of membranes were cast at relative air humidities of 20, 30, 40, and 50%. Representative SEM images of these membranes are provided in

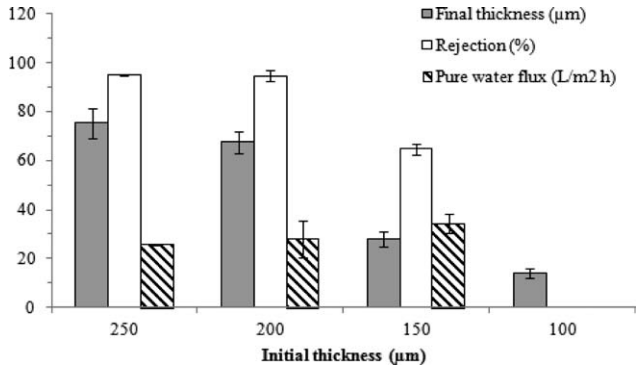

Figure 4 Effect of the initial thickness of the casting film on the performance of the membranes.

Figure 5. The images suggest that the top layers of the membranes cast at relative air humidities of 30, 40, and 50% appeared to have more small, fingerlike macrovoids beneath the surface. On the contrary, the lower relative humidity (20%) produced a denser and less porous structure in the top layer.

If the air humidity is high, the formation process should be considered as a two-stage precipitation process. The impact of the air humidity on the membrane structure in the first stage could be derived from the formation mechanism, which is driven by the concentration gradient in both stages. The availability of water in air (even saturated) is, however, much lower than in the nonsolvent bath. Therefore, if demixing occurs before immersion, the developed hydrodynamic pressures will be much lower than in the nonsolvent bath. This will have two consequences. On one hand, the top layer will be less compacted with the possible absence of a dense skin as a result. On the other hand, this lower compaction will enable the formation of macrovoids very near the surface with an increased probability of the formation of large defects with a large pore size distribution as a result. This hypothesis was partly confirmed by the SEM images. The incidence of small macrovoids (microvoids) near the surface is higher in Figure 5(a) than in Figure 5(d). Differences in skin layer density were not observed but could be derived from the

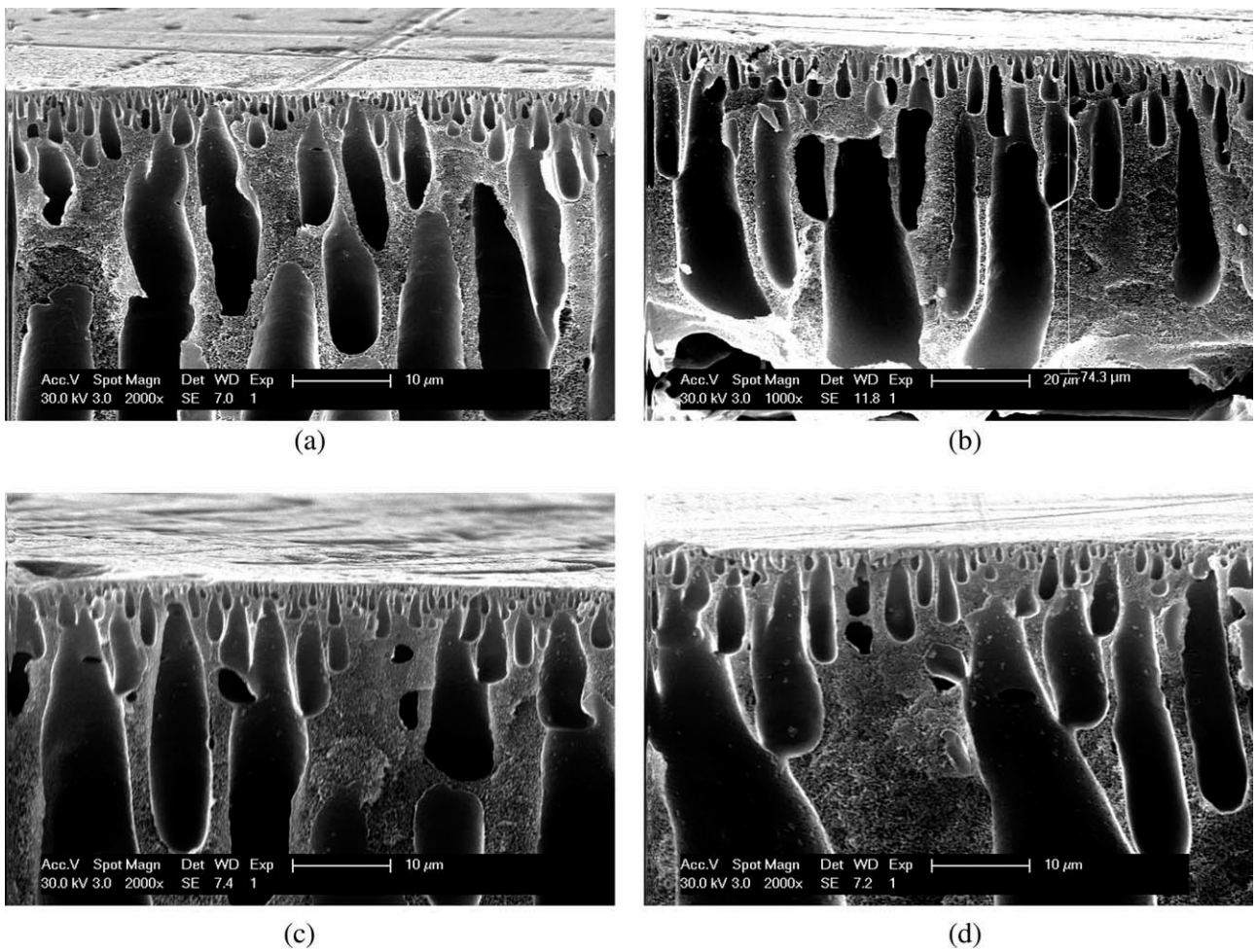

Figure 5 SEM micrographs of membranes synthesized at different relative air humidities: (a) 50, (b) 40, (c) 30, and (d) 20%.

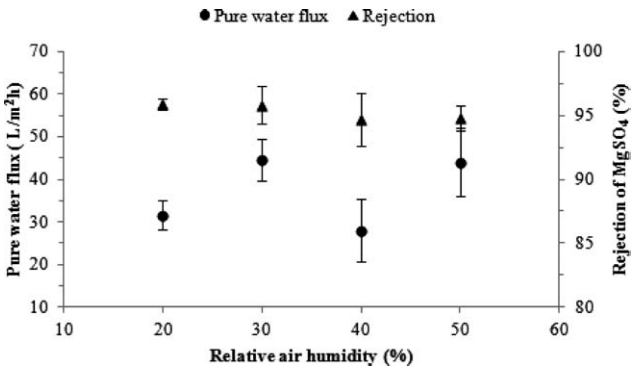

Figure 6 Effect of the relative air humidity on the performance of the membranes.

experimental data (see further). Nevertheless, it could be expected that if the air humidity is large, the formation of the top layer is completely determined in the first precipitation stage. Upon immersion, concentration gradients in the nonsolvent bath would have been lower when a membrane was subjected to high-humidity air. As a result, smaller macrovoids should have formed under the top layer of the membranes that were subjected to high air humidities. This was again confirmed by the SEM images, which showed that the largest macrovoids formed with the lowest air humidity [Fig. 5(d)].

The pure water flux and salt rejection of membranes cast at different relative air humidities are shown in Figure 6. The membranes synthesized at higher relative humidity appeared to give higher pure water flux and lower salt rejection values. However, there was no significant difference among each group. Additionally, the value of standard deviation in each group increased with increasing relative air humidity. This observation suggested that a lower relative humidity enhanced the reproducibility. Boussu et al.[18] also found higher water permeabilities and higher standard deviations on the water permeability for higher air humidity, but they did not provide any explanation for this. As proposed earlier, a high air humidity promoted macrovoid formation very near the surface. This increased the porosity and decreased the mechanical stability of the top layer and resulted in a structure that was more prone to defect formation. The defects were expected to substantially decrease the reproducibility of the experimental data. Although the sublayer of the membrane seemed denser (smaller macrovoids) with higher air humidity, the permeability was found to be higher. The permeability is, however, generally thought to be dominated by the top layer, which in the case of high air humidity, will be less dense and yield a higher permeability. In fact, in industry, water vapor is effectively used to inhibit the formation of a dense skin layer to increase the porosity of the outer layer of hollow-fiber membranes.

Preparation of the ultrathin PA films

Effect of the interfacial polymerization method

In recent research, three methods have been commonly used to perform the interfacial polymerization reaction. These methods, employed in the fabrication of ultrathin PA films, have never been compared before. The methods are as follows: (1) taping a membrane onto a plate with the edges sealed and then immersing it into solutions (method 1),[17,19,22] (2) clipping a membrane between two thick frames and then pouring solutions inside the frame where the solutions come into contact with the active side of the membrane (method 2),[23] and (3) directly immersing a membrane inside solutions with both sides in contact with the solutions (method 3).[3,9,24]

When in contact with the PIP solution, only the active side of the PES membrane was in contact with the solution in methods 1 and 2, but in method 3, the PIP solution could also wet the membrane from the backside. Because of the high solubility of hexane in PES, in the TMC immersion step, the solution could wet all of the membranes very fast. After the excess TMC solution was removed, the membranes of methods 2 and 3 dried very fast because of the high volatility of hexane and the exposed backside of the membrane, but the membrane of method 1 still looked wet. When the three membranes were placed inside an oven without removal of the tools for 8 min, the membranes of methods 2 and 3 were totally dry and flat, but the membrane of method 1 appeared very swollen and had an undulating surface. When the membrane was removed from the glass plate, a lot of hexane vapor came out of the backside. The undulating surface was, therefore, thought to be caused by the vapor pressure of the hexane, which was retained by the membrane. Because of this vapor, the surface morphology looked totally different from those of the other methods, as shown in Figure 7.

Figure 7(a,c) displays the surface morphology of the membrane fabricated by method 1. The surface consisted of white islands separated by darker lines. For the membranes fabricated by methods 2 and 3, the surfaces were similar and uniform, as displayed in Figure 7(b,d). Even at higher magnification [Fig. 7(d)], the membranes made by methods 2 and 3 were smoother and more uniform than that made by method 1 [Fig. 7(c)]. The vapor pressure of the hexane generated lateral tensions in the membrane; this led to the breakup of the thin PA layer when it was formed before swelling or to the formation of PA islands after swelling. The round edges of the islands suggested that the top PA layer was formed after swelling. In any case, method 1 did not allow the formation of a defect-free PA layer.

Figure 8 presents the backside SEM images of the membranes (the backside of the nonwoven fabrics).

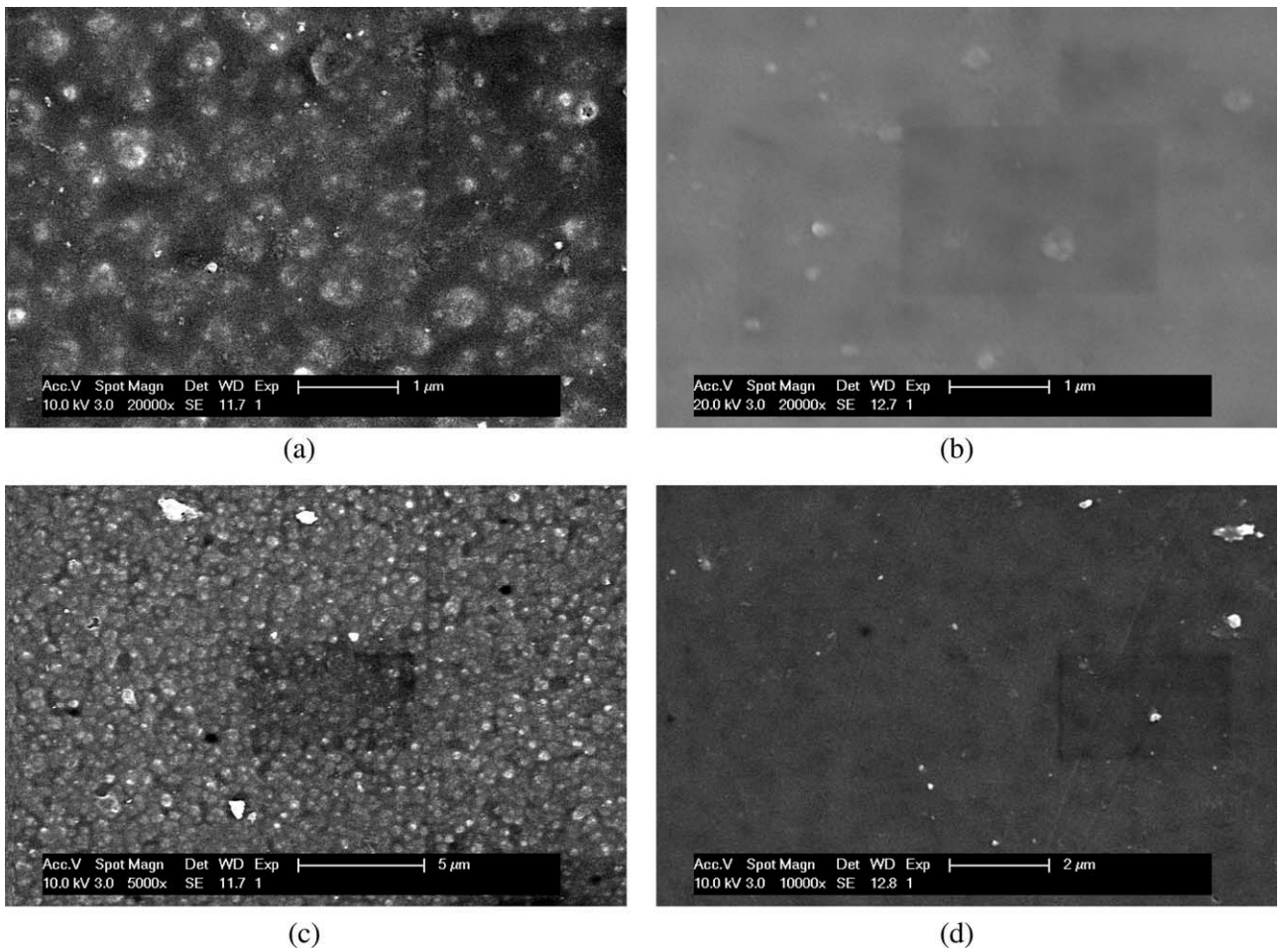

Figure 7 Surface SEM micrographs of the PA membranes fabricated by different interfacial polymerization methods (a,c) surface of the membranes fabricated by tapping on a glass plate and (b,d) surface of membranes fabricated by clamping in frames.

During the PA film fabrication process, in methods 1 and 2, the backside did not come into contact with the solutions. However, in method 3, both sides came into contact the solutions. As shown in Figure 8(a,b), it was obvious that there was a PA layer formed on the backside of the membrane in method 3, as shown in Figure 8(b).

The experimental results for the pure water flux and salt rejection are shown in Figure 9. According to the statistical analysis (ANOVA), the pure water flux from method 2 was significantly higher than the flux values from method 1 ($p < 0.000$) and method 3 ($p < 0.000$), but there was no big difference between methods 1 and 3 ($p < 0.552$). The low flux of method 3 was logical, as two PA layers on the top and the bottom were formed. The low flux for method 1 could be explained by the swelling. Because of the swelling, the solution could more easily enter the PES membrane to form a PA layer inside the PES membrane pores. The tension on the membrane generated by the hexane vapor was released by removal of the membrane from the oven. This yielded a lower flux than would be present in a membrane with a PA layer that was formed without lateral tension (method 2). The salt rejection from method 1 was significantly lower than the rejections from method 2 ($p < 0.000$) and method 3 ($p < 0.036$). This was due to the absence of a defect-free PA layer in method 1. The rejections from methods 2 and 3 were similar ($p < 0.224$).

Effect of the drying method for the removal of the PIP aqueous solution

For the manufacturing of the PA layer, the drying method for the removal of the excess amine (PIP) aqueous solution has never been studied before. Six different drying methods were used in this work: a rubber wiper, a tissue, a cloth, a rubber roller, ambient air, and a compressed air jet. The effect of no drying was also studied. The representative surface SEM images are shown in Figure 10. The performance of these membranes is displayed in Figure 11. To analyze whether there were any significant differences among the methods, ANOVA was performed.

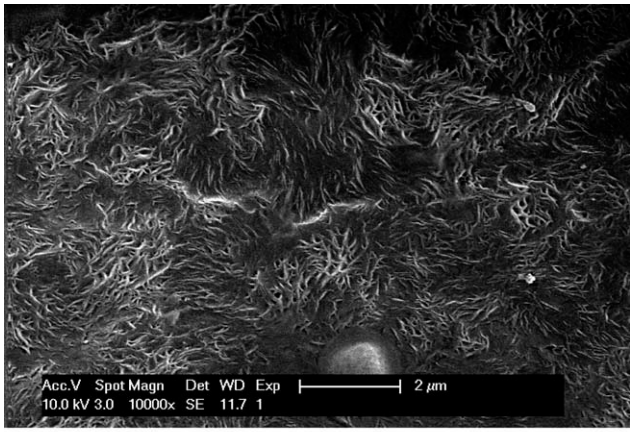

Figure 8 Backside SEM micrographs of the membranes after interfacial polymerization with different methods: (a) membrane without contact with the solutions and (b) membrane with contact with the solutions.

A summary of all of the p values is presented in Table I, where the values with superscripts indicate that the difference in means between two methods was significant.

Figure 10 shows the surface morphologies of the membranes fabricated by different drying methods. Even at low magnification, it was clear that different drying methods gave rise to different surface structures. Figure 11 and Table I prove that the structure and performance of some drying methods were significantly different from others. Figure 10(a1,a2) shows the surface of the PA membrane without any drying step. In the fabrication, after the excess PIP solution was poured out, a relatively thick and uniform PIP solution layer remained on the surface. As a result, the interface between the TMC and the PIP solution formed on a larger distance to the PES support than with other drying methods. Because of this distance, PA growth was not limited to the interface. The PA growth probably even preferentially propagated down toward the PES membrane instead of laterally because of lower growth resistance. This explained the formation of a thick but porous layer with nodular structures. This specific structure generated a high rejection and a significantly higher pure water flux than the membranes dried by ambient air and the compressed air jet, as shown in Figure 11 and Table I.

Figure 10(b1,b2) displays the surface of the PA membrane dried by ambient air. The surface morphology constituted similar nodular structures as seen in the undried membrane [Fig. 10(a2)], but it was less smooth and less uniform. The less uniform structure could be explained in two ways. On one hand, because of the evaporation of water, the PIP monomers tended to aggregate and possibly even crystallize. On the other hand, because of the absence of a water layer, the hexane entered the PES support much more easily. The hexane transported both PIP and TMC monomers toward regions on the support with higher permeabilities. Thereby, both monomers were concentrated and formed a locally thicker PA layer on top or maybe even inside the PES support. This explained not only the less uniform structure but also the much lower fluxes obtained with this drying method (Fig. 11). In Figure 10(h), similar nodular structures can be seen inside some macrovoids near the top layer. The formation of this kind of nodular structure inside the macrovoids during casting of the PES layer is highly unlikely because of the high hydrodynamic pressures and has never been reported before. It is, therefore, suggested that the intrusion of hexane, together with the PIP and TMC monomers into the PES support, created PA nodules even inside the support, with pore blockage as a result.

When a compressed air jet was used to dry the PIP solution, the surface morphology [shown in Fig. 10(c1,c2)] was totally different from those of the last two membranes. In contrast with the nodular structure, Figure 10(c2) shows a large quantity of small spots scattered over the surface. When compressed air was used, most of the PIP solution was blown

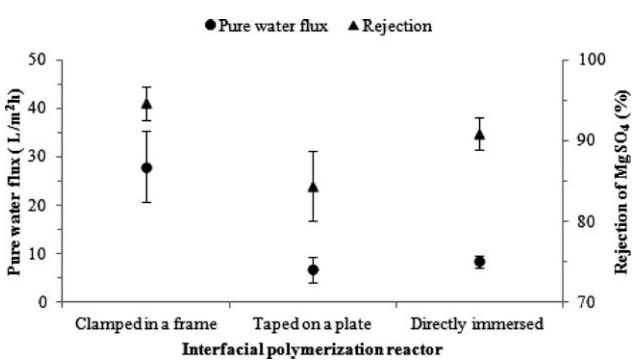

Figure 9 Effect of different interfacial polymerization methods on the performance of the membranes.

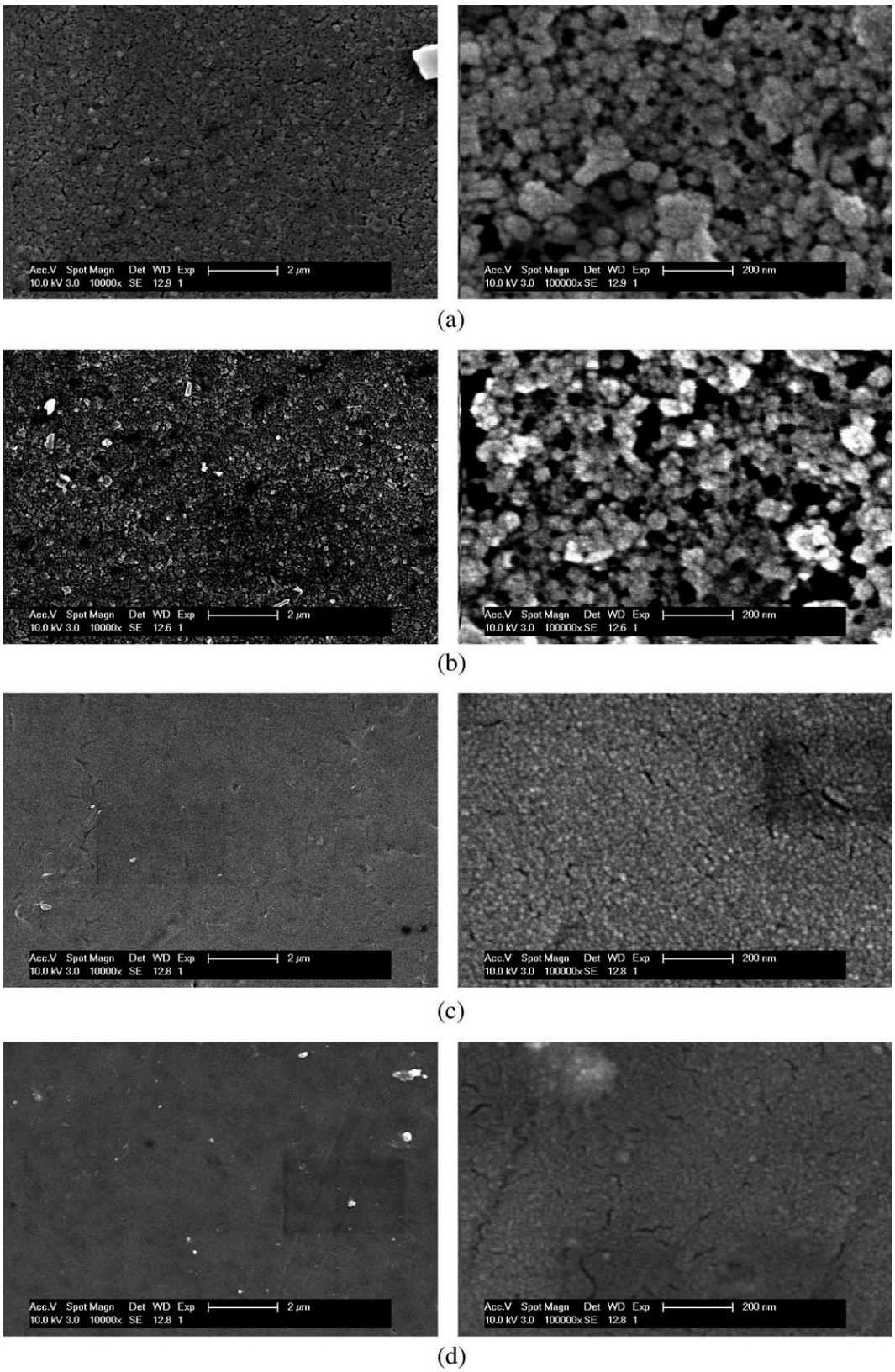

Figure 10 Surface SEM micrographs of the PA membranes fabricated by different drying methods for the removal of the PIP aqueous solution: (a1,a2) without drying or dried with (b1,b2,h) ambient air, (c1,c2) compressed air, (d1,d2) a rubber wiper, (e1,e2) a rubber roller, (f1,f2) a tissue, and (g1,g2) a cloth.

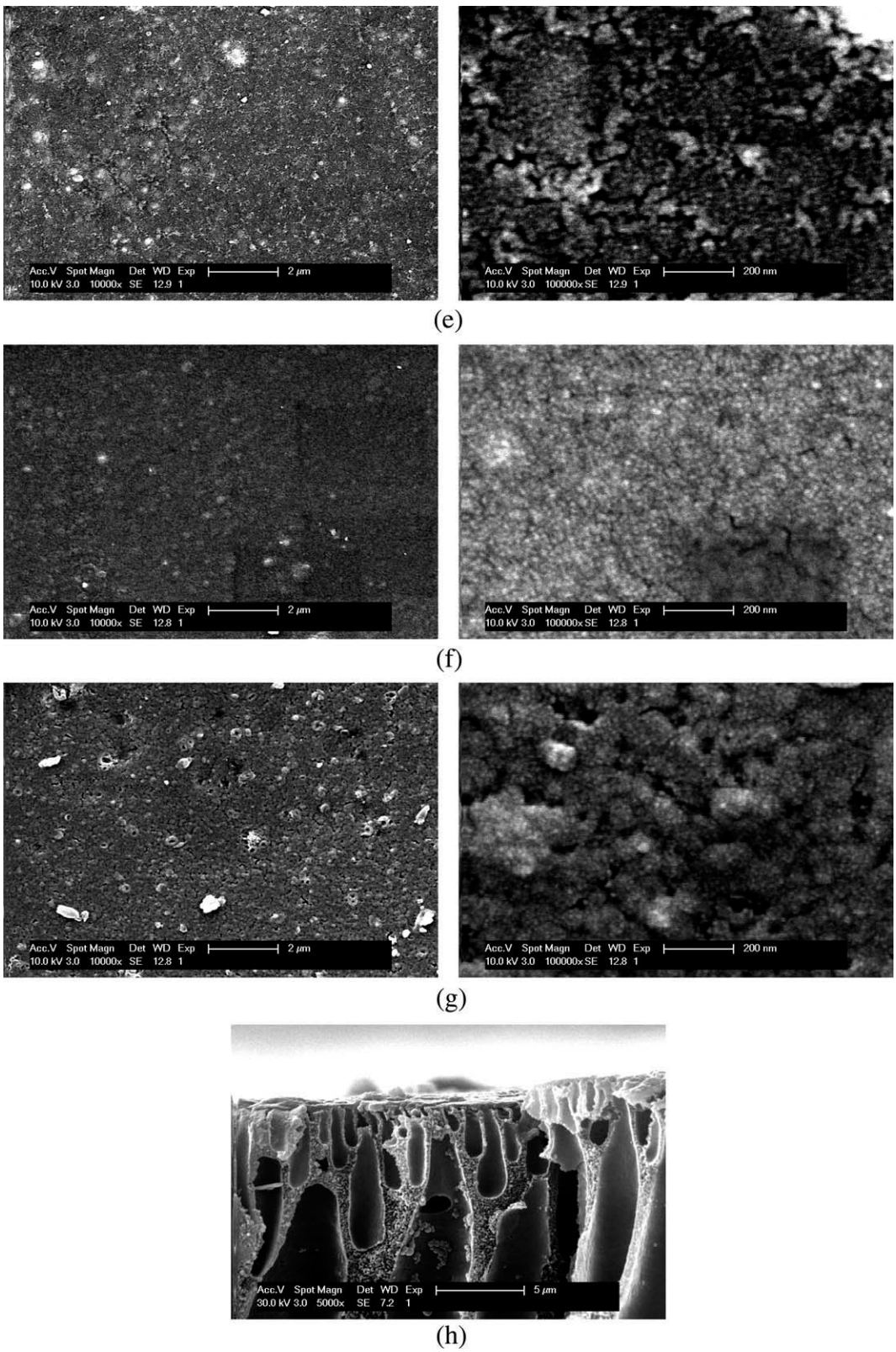

Figure 10 Continued

away. Because of the affinity to the membrane surface, an ultrathin PIP solution film with few monomers was kept on the surface. Because of the pressure generated by the compressed air, some solution might have been pushed into the pores of the surface. Subsequently, TMC reacted with these few PIP monomers on the surface and formed a relatively loose and thin PA layer. As with ambient air drying,

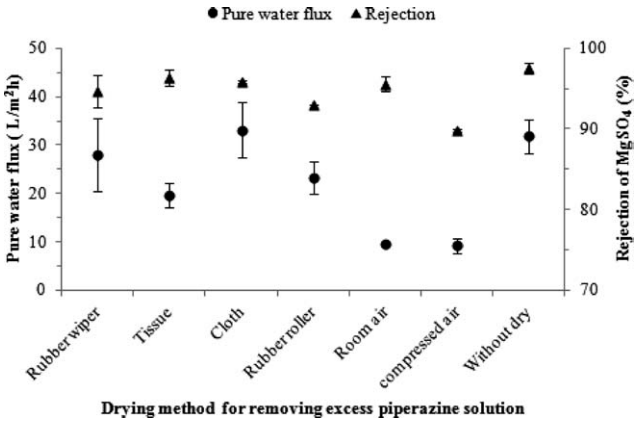

Figure 11 Effect of the drying method for the removal of the PIP aqueous solution.

the absence of water facilitated the entrance of hexane into the PES layer. The PIP inside the pores reacted with TMC and formed PA clusters, which blocked some of the surface pores. The experimental results shown in Figure 11 and Table I reveal that the membrane dried with the compressed air jet had a significantly lower rejection and significantly lower water flux than the membranes dried with most of the other methods. The low rejection was due to the loose and ultrathin PA layer, and the low flux was caused by pore blockage by PA nodules.

Compared with the two air-drying methods, the rubber wiper retained a uniform and thin aqueous PIP layer and decreased the chance of hexane intrusion into the PES support. This was confirmed by the higher flux (Fig. 11). Because of the thinner water layer compared to that with any other drying method, the PA layer tended to grow more laterally and, thereby, created a denser structure. Although the difference was not significant, a lower flux was observed compared to that without drying (Fig. 11).

From the remaining drying methods (rubber roller, tissue, and cloth), the tissue had a more uniform water-absorbing capacity, with a more uniform PA layer as a result [Fig. 10(f2)]. Although there was a slight difference between each surface image, according to the experimental results and the statistical analysis, there were no significant differences among these methods.

From the previous analysis, it is clear that a uniform aqueous PIP layer was absolutely essential for preventing hexane intrusion in the PES layer and for obtaining a uniform PA layer with a high flux and rejection. We concluded that the omission of the drying step yielded the simplest procedure without a significant loss of performance.

Effect of the curing time

Curing (or heating) is crucial for promoting further crosslinking by dehydration of the unreacted amine and carboxyl groups and for removing residual solvent. The optimal curing conditions for different solvents depend on the solvent evaporation rate (i.e., boiling point).[3] Ghosh et al.[3] reported that increases in the curing temperature (45 and 90°C) gave rise to additional crosslinking, which resulted in a higher salt rejection. The tested temperatures were far from the boiling point of hexane (69°C). Also, only short timescales were investigated, and no standard deviation was presented. So to further investigate the influence of the curing time on the performance, our membranes were synthesized at 60°C and cured for 0, 2, 8, 16, and 24 min, respectively. The results of the water flux and salt rejection for each curing time

TABLE I
***p* Values from Different Drying Methods for the Removal of the PIP Aqueous Solution**

Flux	A	B	C	D	E	F	G
A		0.048[a]	0.04[a]	1	0.964	0.668	1
B	0.048[a]		1	0.026[a]	0.519	0.892	0.031[a]
C	0.04[a]	1		0.021[a]	0.464	0.852	0.026[a]
D	1	0.026[a]	0.021[a]		0.999	0.793	0.996
E	0.964	0.519	0.464	0.999		1	0.893
F	0.668	0.892	0.852	0.793	1		0.52
G	1	0.031[a]	0.026[a]	0.996	0.893	0.52	
Rejection	A	B	C	D	E	F	G
A		0.987	0.005[a]	0.478	0.219	1	0.999
B	0.987		0.064	1	0.91	1	1
C	0.005[a]	0.064		0.03[a]	0.74	0.023[a]	0.041[a]
D	0.478	1	0.03[a]		0.966	0.972	0.999
E	0.219	0.91	0.74	0.966		0.617	0.797
F	1	1	0.023[a]	0.972	0.617		1
G	0.999	1	0.041[a]	0.999	0.797	1	

A, without drying; B, dried with ambient air; C, dried with peripheral air; D, dried with a rubber wiper; E, dried with a rubber roller; F, dried with a tissue; G, dried with a cloth.

[a] The mean difference was significant at the 0.05 level.

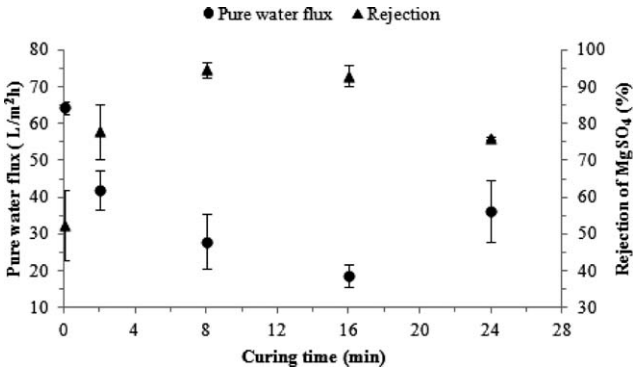

Figure 12 Effect of the curing time on the performance of the PA membranes.

are plotted in Figure 12. The cross-sectional images are similar to those in Figure 1(a).

The water flux decreased in the curing time range of 0–16 min but increased at 24 min. However, the salt rejection increased from 0 to 16 min but dropped off at 24 min. With increasing curing time, further evaporations of hexane, water, and acid (generated by dehydration) were achieved. The unreacted TMC and PIP monomers were exposed and had a chance to come into contact with each other; this resulted in more PA formed and more crosslinking achieved. Additionally, because of the additional reaction, either the thickness or the density of the PA layer increased. Regardless of which situation occurred, the water flux decreased and the salt rejection increased with increasing degree of crosslinking. The similar cross-sectional images of these membranes suggested that curing at 60°C within 24 min could not change the support membrane structure. The performance of the membrane cured for 24 min indicated that a significantly longer curing time may lead to shrinkage of the PA layer. Because the PA layer was ultrathin and uniform, as discussed in the previous section, shrinkage may have caused some defect in the PA layer and resulted in a higher flux and lower rejection. We concluded that at 60°C, a curing time of 8 min was optimal.

CONCLUSIONS

In this article, we have presented a systematic and detailed investigation of the relationship between the manufacturing conditions of both the PES support layer and the PA top layer of a TFC membrane and the resulting membrane structures and performance. The PA layer was synthesized by interfacial polymerization, and the PES support layer was formed by immersion precipitation.

For the PES support layer, the effect of the wetting pretreatment, initial casting film thickness, and relative air humidity were investigated. A new understanding was gained from the SEM images and experimental data. Because of the flux, a wetting pretreatment is not recommended. Wetting can decrease the concentration gradient and result in a sublayer structure with smaller macrovoids and, thus, a lower flux. To limit polymer intrusion into the nonwoven support, an increase in casting speed is needed. Decreasing the casting thickness to a certain level did not significantly influence the performance of the membranes but resulted in important polymer savings. However, below this level, the mechanical stability and integrity of the membrane could not be assured, especially when a nonwoven support with a high roughness was used. Another important finding was that the air humidity during casting influenced the formation of a dense, defect-free skin layer. A high air humidity promoted macrovoid formation very near the surface of the membrane and compromised the formation of a dense, defect-free skin layer during casting. These defects significantly reduced the reproducibility of the process.

For the PA layer, the interfacial polymerization method, the drying method, and the curing time were studied. The clamping of the membrane in a frame was found to be the best method; it yielded the best performance of membranes and conserved the dosage of the PIP and TMC solutions. The taping of the membrane to a glass plate resulted in lateral tension during curing by hexane vapor pressure trapped on the backside. Because of this tension, it was difficult for a uniform PA layer, and the formation of PA inside the pores was promoted. Because some methods caused the absence of a uniform PIP solution layer, nodular PA structures were found inside the macrovoids of the PES layer. From this observation, we derived that if not enough water was present for interfacial polymerization, hexane, together with TMC and PIP, entered the PES sublayer, and pore blockage by PA formation occurred; this resulted in a dramatic decrease in the flux. Moreover, according to the experimental data, a drying step is not a prerequisite; this enhances the ease of operation. Finally, a curing time of 8 min was found to be optimal in this work. Enough time was necessary to increase the amount of crosslinking. Longer curing times resulted in PA layer shrinkage, with defect formation as a result.

References

1. Petersen, R. J. J Membr Sci 1993, 83, 81.
2. Chen, S. H.; Chang, D. J.; Liou, R. M.; Hsu, C. S.; Lin, S. S. J Appl Polym Sci 2002, 83, 1112.
3. Ghosh, A. K.; Jeong, B. H.; Huang, X.; Hoek, E. J Membr Sci 2008, 311, 34.
4. Manttari, M.; Nuortila-Jokinen, J.; Nystrom, M. J Membr Sci 1997, 137, 187.
5. Sridhar, S.; Kale, A.; Khan, A. J Membr Sci 2002, 205, 83.
6. Sridhar, S.; Prasad, K. K.; Murthy, G. S.; Rao, A. G.; Khan, A. A. J Chem Technol Biotechnol 2003, 78, 1061.

7. Joshi, S.; Ghosh, P.; Shah, V.; Devmurari, C.; Trivedi, J.; Rao, P. Desalination 2004, 165, 201.
8. Turan, M. Desalination 2004, 170, 83.
9. Ghosh, A. K.; Hoek, E. J Membr Sci 2009, 336, 140.
10. Mulder, M. Basic Principles of Membrane Technology; Kluwer Academic Publishers: Dordrecht, the Netherlands, 1996.
11. Barth, C.; Goncalves, M.; Pires, A.; Roeder, J.; Wolf, B. J Membr Sci 2000, 169, 287.
12. Kim, J. H.; Lee, K. H. J Membr Sci 1998, 138, 153.
13. Han, M. J. Desalination 1999, 121, 31.
14. Baik, K. J.; Kim, J. Y.; Lee, J. S.; Kim, S. C.; Lee, H. K. Korea 2001, 9, 285.
15. Chaturvedi, B.; Ghosh, A.; Ramachandhran, V.; Trivedi, M.; Hanra, M.; Misra, B. Desalination 2001, 133, 31.
16. Han, M. J.; Nam, S. T. J Membr Sci 2002, 202, 55.
17. Ahmad, A.; Ooi, B.; Wahab Mohammad, A.; Choudhury, J. J Appl Polym Sci 2004, 94, 394.
18. Boussu, K.; Vandecasteele, C.; Van der Bruggen, B. Polymer 2006, 47, 3464.
19. Saha, N.; Joshi, S. J Membr Sci 2009, 342, 60.
20. Prakash Rao, A.; Desai, N.; Rangarajan, R. J Membr Sci 1997, 124, 263.
21. Prakash Rao, A.; Joshi, S.; Trivedi, J.; Devmurari, C.; Shah, V. J Membr Sci 2003, 211, 13.
22. Jeong, B. H.; Hoek, E.; Yan, Y.; Subramani, A.; Huang, X.; Hurwitz, G.; Ghosh, A. K.; Jawor, A. J Membr Sci 2007, 294, 1.
23. Lee, H. S.; Im, S. J.; Kim, J. H.; Kim, H. J.; Kim, J. P.; Min, B. R. Desalination 2008, 219, 48.
24. Rahimpour, A.; Jahanshahi, M.; Mortazavian, N.; Madaeni, S. S.; Mansourpanah, Y. Appl Surf Sci 2010, 256, 1657.